DESIGN, ANALYSIS, AND TESTING OF HIGH PERFORMANCE BEARINGS IN A HIGH SPEED INTEGRALLY GEARED COMPRESSOR

by

Wen Jeng Chen

Senior Engineering Consultant

Ingersoll-Rand Company

Mayfield, Kentucky

Fouad Y. Zeidan

Director of Engineering

and

Dilip Jain

Senior Project Engineer

KMC, Inc.

West Greenwich, Rhode Island

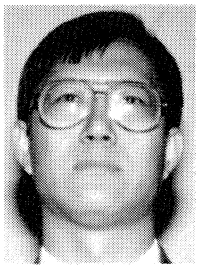

Wen Jeng Chen is a Senior Engineering Consultant with Ingersoll-Rand Company, Centrifugal Compressor Division, in Mayfield, Kentucky. He is responsible for providing technical support for the development, design and analysis of mechanical components of centrifugal compressors. He conducts research and development in the areas of rotordynamics, lubrication, and bearing design. Dr. Chen received his M.S. (1984) and Ph.D. (1987) degrees in Mechanical Engineering from Arizona State University. He is a member of ASME.

Fouad Y. Zeidan is Director of Engineering at KMC, Inc., in West Greenwich, Rhode Island. Prior to joining KMC, Dr. Zeidan held positions at Amoco Research Center, IMO Industries CentriMarc Division, and Qatar Fertilizer where he worked in maintenance and troubleshooting of rotating machinery, bearing design and failure analysis, vibration analysis, rotordynamic analysis, upgrading of critical plant equipment, and auditing of new machinery. At KMC, he is working on the design and development of radial and thrust bearings for oil, process, and gas lubricated applications. He has published over 25 technical papers and articles on various turbomachinery topics. He has several patent filings for an integral squeeze film centering spring damper and other high performance journal and thrust bearings. He received his B.S.M.E. (1978), M.S.M.E. (1979), and Ph.D. (1989) degrees from Texas A&M University.

Dilip Jain is Senior Project Engineer at KMC, Inc., in West Greenwich, Rhode Island. Mr. Jain is actively involved in the design, analysis, and testing of journal and thrust bearings using conventional and process lubricants. He is in charge of the testing and development of polymer and nonmetallic bearing grade materials. Mr. Jain developed parametric design computer programs for the efficient and optimal design of journal bearings, thrust bearings, and squeeze film dampers. Prior to joining KMC, Mr. Jain worked at Schwitzer, Inc., where he designed turbocharger turbines and compressors for improved inertia and efficiency. He was also responsible for developing variable geometry turbochargers and the algorithms for its electronic control to improve response, efficiency, and emission. He obtained his Bachelors degree (1982) in Mechanical Engineering from the Indian Institute of Technology, and his Masters degree (1983) from Villanova University. He has published and presented papers at ASME, SAE, IMechE, and ANSYS Conferences. He is an associate member of ASME, and a member of Tau Beta Pi.

ABSTRACT

Analysis, design, and optimization of high performance journal and thrust bearings in a high speed integrally geared compressor are described. The high speed and relatively small bearing size stretches the applicable limits of conventional style tilt pad bearings. The variation in the load magnitude, as is the case with most gear loaded bearings, requires careful analysis of the stability and unbalance response characteristics. An optimized new flexible pivot bearing was used in this application to provide stable operation throughout the wide ranges of load and inlet temperature. The bearing incorporated a directed lubrication feature to reduce the hot oil carry over which is known to be a major contributor to high bearing temperatures in high speed applications. The precision inherent in the manufacturing process used to produce this style of bearing allowed further optimization of the preload and pivot offset. The use of an offset

pivot configuration demonstrated lower sensitivity to bearing clearance variation.

The necessity for high rotational speeds in integrally geared compressors increases the frictional power losses in the journal and thrust bearings. The parasitic losses constitute a significant percentage of the overall bearing power losses. Bearing designs that were utilized to reduce both the frictional and parasitic losses in the thrust bearings are discussed. The new thrust bearings were designed to provide an optimum crown-to-film thickness ratio allowing the bearing to carry the design thrust load with fewer pads. The analytical results for the conventional and deflection journal and thrust bearings are presented and compared to the test data. The new bearing resulted in lower steady state vibrations. At surge conditions, the synchronous and subsynchronous vibrations were about 25 percent of the conventional tilt pad bearing. The frictional and parasitic power losses with the new thrust bearing were about 20 percent lower than those of the conventional bearings. The temperature rise was also lower which indicated that the inlet temperature can be further increased with the new bearing allowing a wider operating temperature range and lower frictional losses.

INTRODUCTION

The trend in integrally geared compressors is towards high performance and efficiency, high reliability, and lower maintenance. In order to achieve the high performance and aerodynamic efficiency in radial flow impellers, high rotating speeds are essential. The higher speeds and lighter shafts tend to make the machines more rotordynamically sensitive. The problems are compounded in the case of integrally geared compressors, where the gear drive arrangement results in an overhung impeller with its inherently higher aerodynamic cross coupling. This subsequently presses the bounds of the stability limits.

The services demanded from these compressors mandates robust and reliable operation at a relatively wide range of bearing loads and oil inlet temperatures. The aerodynamic stage efficiency requirements limits the axial float to a maximum of five mil. Therefore, reducing the power loss in the bearings is essential in order to maintain the high compressor stage efficiency. Higher speeds, increased rotor flexibility, and variations in the bearing gear load magnitude, coupled with the demand for lower frictional and parasitic losses necessitate an in depth bearing design and analysis process.

The two stage integrally geared air compressor shown in Figure 1 was the focus of this design investigation. The compressor was developed using agile engineering described by Japikse and Olsofka [1] and represents the state of the art in integrally geared compressors. The driver is a flange-mounted induction motor. The drive train is shown in Figure 2 and consists of a bull gear, an intermediate gear, and the high speed pinion shaft carrying two overhung impellers. The maximum rated pinion speed is 76,500 rpm and is expected, with further development, to reach even 20 to 30 percent higher speeds. The high speed pinion shaft shown in Figure 3 is supported by two combination radial thrust bearings. The bearings are of one piece (unsplit) configuration.

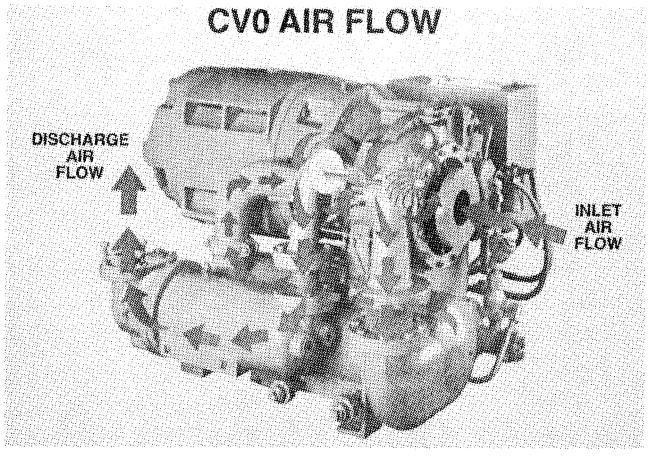

Figure 1. Two Stage Integrally Geared Air Compressor.

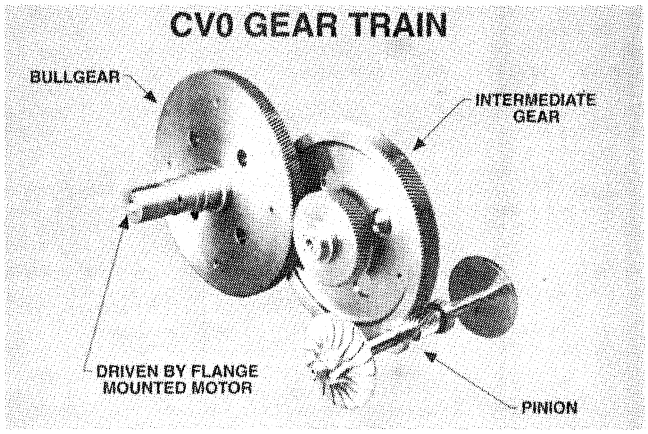

Figure 2. CV0 Gear Drive Train.

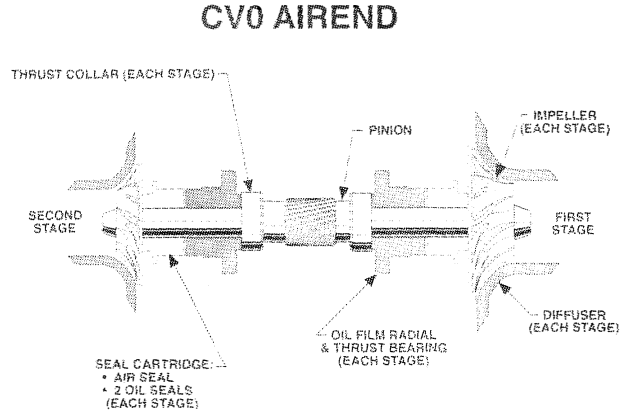

Figure 3. Schematic of Rotor Configuration.

ROTORDYNAMIC ANALYSIS AND BEARING OPTIMIZATION

Undamped Critical Speed Analysis

A computer generated rotor model for the high speed pinion shaft is shown in Figure 4. The undamped critical speed map as a function of support stiffness is shown in Figure 5. The equivalent dynamic stiffness coefficients for the conventional five pad tilting pad bearing (TPB) are shown as a function of speed and are superimposed on the undamped critical speed map. The coefficients intersect the first two rigid body critical speeds and the first flexible mode in the sloping section of the curves. This ensures that there is significant motion at the bearings to help dampen the shaft motion as the rotor traverses the critical speeds when accelerating to the operating speed. The coefficients for the optimized four pad flexible pivot bearing (FPB) are also superimposed on the critical speed map as shown in Figure 5.

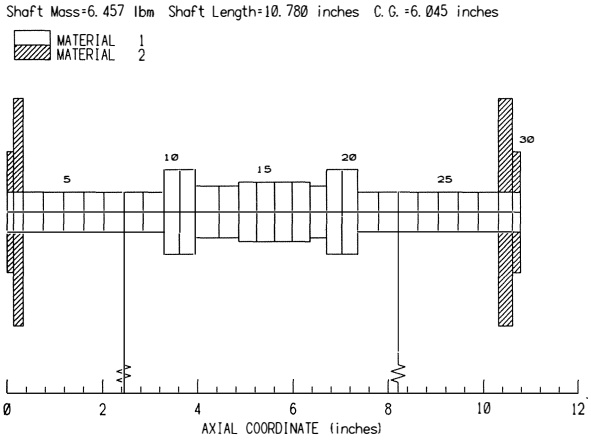

Figure 4. Computer Generated Rotordynamic Model.

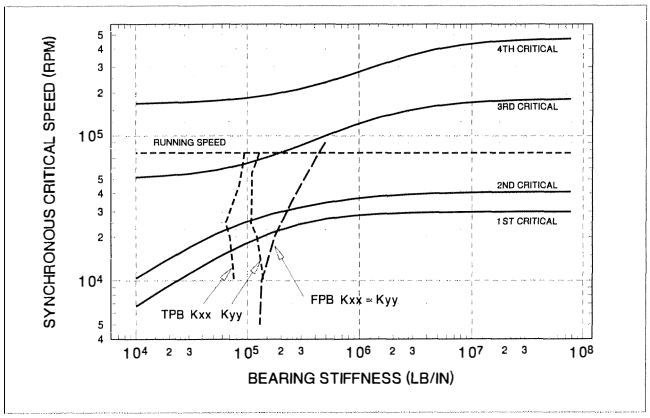

Figure 5. Undamped Critical Speed Map.

This bearing has an offset pivot which was chosen, as will be shown later, for its superior stability characteristics over a wider range of bearing clearances. The offset pivot configuration also provides higher stiffness in the bearing and helps shift the third mode further away from the running speed. This is later verified through the stability and unbalance response analysis.

Journal Bearing Design and Analysis

The calculations performed to determine the minimum and maximum clearances and preload at the extremes of the manufacturing tolerances are shown in Table 1. The conventional style tilt pad bearing, as shown, will have a rather wide range in clearance and preload. This is inherent in the design and assembly of these bearings that results from the stackup of the manufacturing tolerances for the individual parts making the bearing assembly. This is the reason why many of these bearings very often have a high preload value. The high preload value is required to counter the negative effects of the manufacturing tolerances that can otherwise result in a negative preload condition. Another complication that affects bearing design, and is characteristic of most gear loaded bearings, is the variation in the bearing load from partial load to full load conditions. This requires the bearing to have a wide range of stable operation under partial and full load conditions.

In order to accentuate some of the differences between the two bearing styles examined in this investigation, it is essential to describe the manufacturing method and techniques used in producing the flexible pivot bearings. These bearings are fabricated using wire electric discharge machining (EDM) while they are submerged in water during this process. The water is maintained at a constant temperature which is typically held within 1°F of the room temperature, to ensure thermal stability during the cutting process. The back of the pad and the web (pivot) are cut first, then the part is released to allow it to relax. The part is then reclamped and the final bore is cut in the last step. This ensures that the effect of any pad rotation is completely eliminated. Since the pad and bearing shell are one piece, tolerance stackup is also eliminated. As shown in Figure 6, the set bore and pad bore are cut in one operation, further reducing the manufacturing tolerance. The set bore and the pad machined bore are not independently generated, as is the case with the conventional style tilt pad bearings. This further reduces the resulting preload spread for the FPB as shown in the right column of Table 1. The radial and thrust bearing subassemblies are shown in Figure 7. The wire EDM machine used in the manufacture of the radial bearings is capable of cutting the set bore to within 0.0001 in, which is difficult to measure even with most electronic coordinate measuring machines (CMM). With this manufacturing method, there is no need for subsequent assembly and checking, which can be very time consuming with conventional style bearings. Note that in order to maintain a preload of 0.2, the drop off, as shown in Figure 8, from the center of the pad to the edge is about 0.000213 in to 0.000493 in, which would be impossible to achieve without the high precision and accuracy of state-of-the-art wire EDM machines. The material between the pads is utilized as integral directed lubrication nozzles, and the material left underneath the pads provides squeeze film damping.

Table 1. Calculation of Minimum and Maximum Preload.

Conventional Tilt Pad Bearing	*Flexible Pivot Bearing*
$\text{Journal Diameter}_{min} = 0.8198$	$\text{Journal Diameter}_{min} = 0.8198$
$\text{Journal Diameter}_{max} = 0.8200$	$\text{Journal Diameter}_{max} = 0.8200$
$\text{Pad Set Bore}_{min} = 0.8230$	$\text{Pad Set Bore}_{min} = 0.8224$
$\text{Pad Set Bore}_{max} = 0.8238$	$\text{Pad Set Bore}_{max} = 0.8228$
$\text{Pad Machined Bore}_{min} = 0.8234$	$\text{Pad Machined Bore}_{min} = 0.8232$
$\text{Pad Machined Bore}_{max} = 0.8243$	$\text{Pad Machined Bore}_{max} = 0.8236$
$\text{Preload} = m = 1 - \frac{C_b}{C_p} = 1 - \frac{D_b - D_j}{D_b - D_j}$	
$\text{Preload}_{min} = 1 - \frac{D_{bmax} - D_{jmin}}{D_{pmin} - D_{jmin}}$	$\text{Preload}_{min} = \frac{D_{dmax} - D_{bmax}}{D_{pmax} - D_{jmin}}$
$\text{Preload}_{max} = 1 - \frac{D_{bmin} - D_{jmax}}{D_{pmax} - D_{jmax}}$	$\text{Preload}_{max} = \frac{D_{pmin} - D_{bmin}}{D_{pmin} - D_{jmax}}$
$m_{min} = 1 - \frac{0.8238 - 0.8198}{0.8234 - 0.8198}$	$m_{min} = \frac{0.8236 - 0.8228}{0.8236 - 0.8198}$
$m_{min} = \boxed{-0.1000}$	$m_{min} = \boxed{0.2105}$
$m_{max} = 1 - \frac{0.8230 - 0.8200}{0.8243 - 0.8200}$	$m_{max} = \frac{0.8232 - 0.8224}{0.8232 - 0.8198}$
$m_{max} = \boxed{0.3023}$	$m_{max} = \boxed{0.2352}$
$m_{nom} = 1 - \frac{0.8234 - 0.8199}{0.82385 - 0.8199}$	$m_{nom} = \frac{0.8234 - 0.8226}{0.8234 - 0.8199}$
$m_{nom} = \boxed{0.1139}$	$m_{nom} = \boxed{0.2285}$

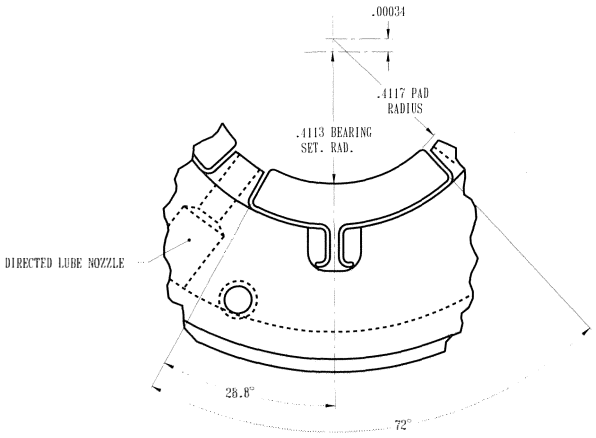

Figure 6. Schematic of the Flexure Pivot™ Bearing.

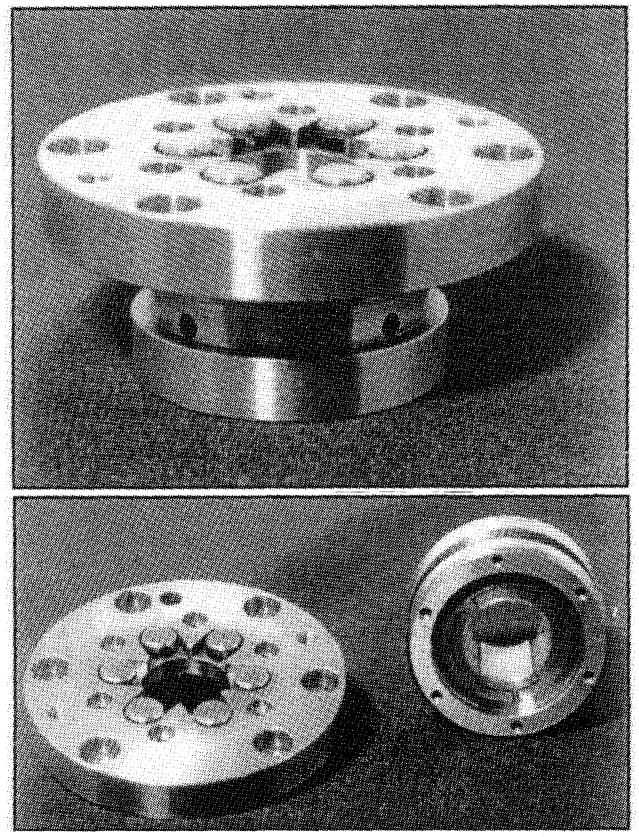

Figure 7. Radial and Thrust Bearing assemblies.

Stability Analysis

The first three forward modes with the conventional tilt pad bearings at the maximum preload conditions are shown in Figures 9, 10, and 11, respectively. Note that, as depicted in the undamped critical speed map, the third forward mode is around 60,000 rpm and is below the running speed. The first forward mode with the conventional tilt pad bearings at the minimum preload conditions is shown in Figure 12. Note that the logarithmic decrement (log dec) of the first forward mode drops by about 22 percent in comparison to the log dec at the maximum preload conditions. The minimum preload condition is also very susceptible to pad flutter due to the fact that the pads can possibly operate with a negative preload.

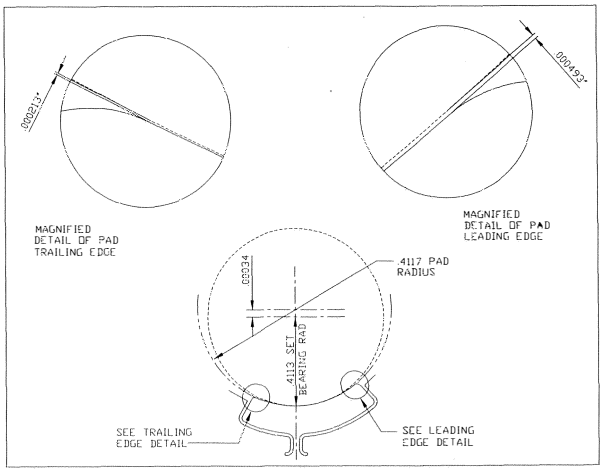

Figure 8. Precision Needed for Obtaining the Drop-off at the Leading and Trailing Edges.

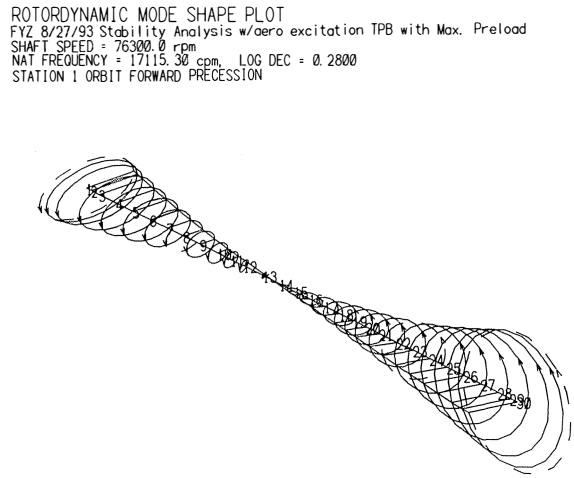

Figure 9. First Forward Mode with the Conventional Tilt Pad Bearings (Maximum Preload).

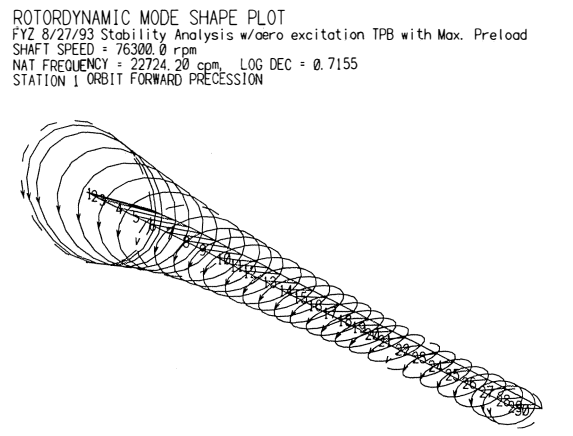

Figure 10. Second Forward Mode with the Conventional Tilt Pad Bearings (Maximum Preload).

The stability analysis was also performed with the flexible pivot bearings. The first three forward modes with a set of optimized four pad flexible pivot bearings are shown in Figures

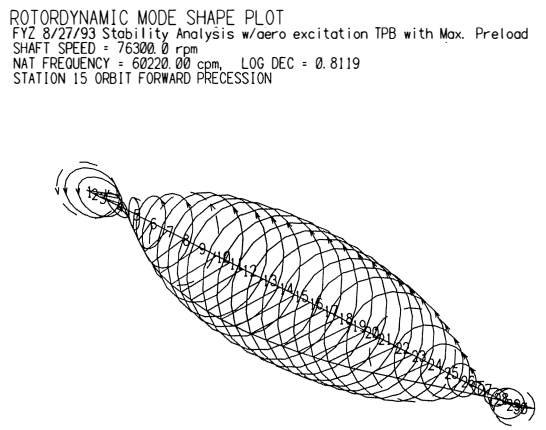

Figure 11. Third Forward Mode with the Conventional Tilt Pad Bearings (Maximum Preload).

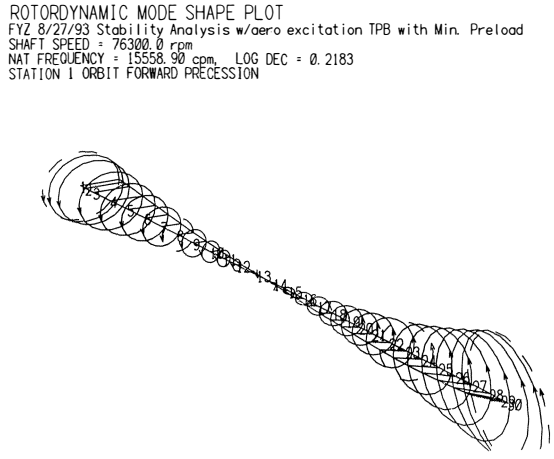

Figure 12. First Forward Mode with the Conventional Tilt Pad Bearings (Minimum Preload).

13, 14, and 15, respectively. Note that in this case the first forward mode has a logarithmic decrement 30 to 50 percent better than that achieved with the conventional tilt pad bearing. The third mode is also above the running speed and is well

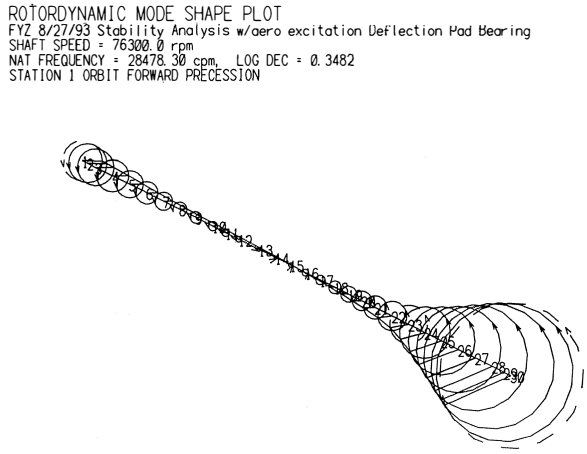

Figure 13. First Forward Mode with the Optimized Four Pad Flexure Pivot Bearing.

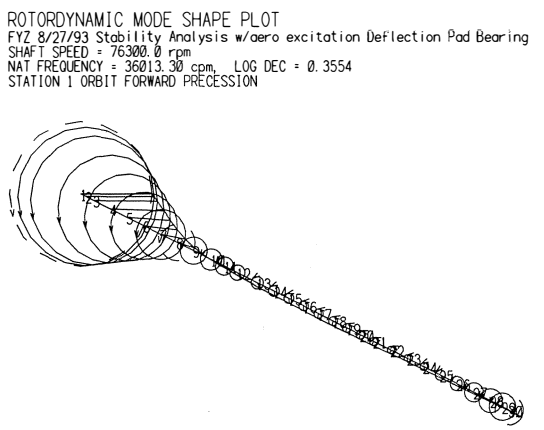

Figure 14. Second Forward Mode with the Optimized Four Pad Flexure Pivot Bearing.

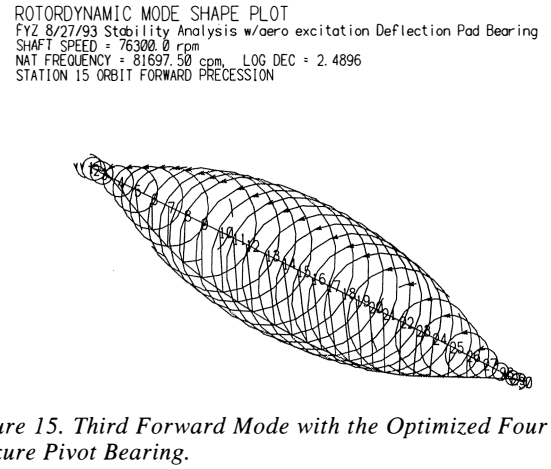

Figure 15. Third Forward Mode with the Optimized Four Pad Flexure Pivot Bearing.

damped with a log dec of 2.489. The ability to manufacture the bearing with a relatively low preload, and to maintain the minimum and maximum variations due to manufacturing tolerances very close to the target value is a great advantage in this application.

In order to demonstrate the high reliability over a long period of operation, the analysis was also conducted at a slightly higher set bore clearance (3.2 mil). This was performed to evaluate the effect of wear on the bearing in services that may require many starts and stops, and also to examine future applications where the speed may possibly increase from 20 to 30 percent over the current operating speed. The higher speeds will require the larger clearance to guard against bearing seizure. The results of this investigation are shown in Table 2. Note that the five pad configuration with the 0.5 pivot offset resulted in a negative logarithmic decrement for the first forward mode. Using a pad offset of 0.6 increased the stability margin (log dec = 0.186), but it continued to show sensitivity to bearing clearance with the five pad bearing. The four pad bearing with a 0.5 offset offered much better stability at 2.4 mils clearance (log dec = 0.38). However, there was a drastic reduction in stability (log dec = -0.241) when the clearance was increased to 3.2 mils. A four pad bearing with an offset pivot of 0.6 provided better overall stability at both clearances as shown in Table 2. What is of importance in this optimization process is the fact that an offset pivot design reduced the sensitivity of the bearing to clearance variations. The offset pivot, as shown on the undamped critical

Table 2. Summary of the Stability Analysis Flexible Pivot Bearing.

# of Pads	*Offset*	*Preload*	*Dia. Clr. (Mils)*	*First Forward Mode*
5	0.5	0.2	3.2	-0.443
5	0.5	0.2	2.4	-0.290
4	0.5	0.2	3.2	-0.241
4	0.5	0.2	2.4	0.380
5	0.6	0.2	3.2	-0.007
5	0.6	0.2	2.4	0.186
4	0.6	0.2	3.2	0.249
4	0.6	0.2	2.4	0.348

speed map, also helped slant the equivalent dynamic bearing stiffness to the right, avoiding traversing the third critical speed.

There are other advantages that also can be realized with an offset pivot design. The maximum film temperature is one of the primary limiting parameters with gear loaded bearings running at high speeds. The offset pivot can significantly help reduce that temperature. This is shown in Figure 16 for both the five and four pad bearings at 0.6 pivot offset compared to the 0.5 offset values. There is a 20 to 30°F drop in the operating temperature with an offset pivot. The directed lubrication nozzles serve to further reduce the operating temperatures. Inhouse testing at the bearing manufacturer's test facilities showed that directed lubrication significantly reduces the hot oil carry over from one pad to the next. This can also result in reducing the maximum operating temperatures by about 25 to 30°F.

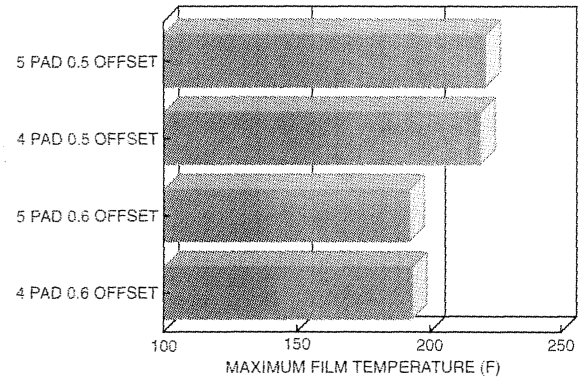

Figure 16. Maximum Film Temperature for Different Bearing Configurations.

Unbalance Response Analysis

Unbalance response analysis was computed with the conventional tilt pad bearing at both extremes of the manufacturing tolerances (minimum and maximum preload). The response with the optimized flexible pivot bearing is also shown on the same plot in Figure 17. The response at operating speed is about 50 percent lower with the flexible pivot bearing, compared to the conventional tilt pad bearings. Note that the response is still very low at the higher speeds projected for future machines. The peak response, due to the critical speed at 60,000 rpm with the conventional tilt pad bearing, is eliminated with the optimized flexible pivot bearing.

Design and Stress Analysis of the Radial FPB Bearing

An ANSYS® model of the pad geometry was generated for the purpose of determining the rotational stiffness of the pad and the

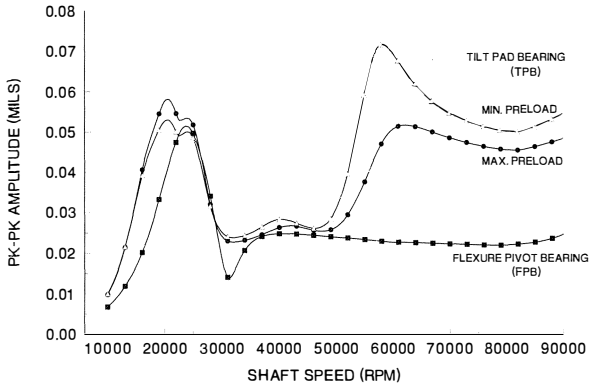

Figure 17. Unbalance Response Predictions with the Two Bearing Configurations.

location of the pivot in the structure. The bearing is then analyzed at the maximum static gear load to compute the static tilt or flexure. A stress contour plot of the stresses in the pad due to static loading is shown in Figure 18. The unbalance response analysis is then used to determine the dynamic loads transmitted from the rotor to the bearing. Using the stress results at static and dynamic conditions, one is able to compute the Modified Goodman diagram shown in Figure 19. The safety factor can then be determined from the information shown in the figure. Note that the dynamic load is calculated using eight times the maximum unbalance value specified in API 617 Fifth Edition. Even with this high unbalance value, the safety factor is over 12.5.

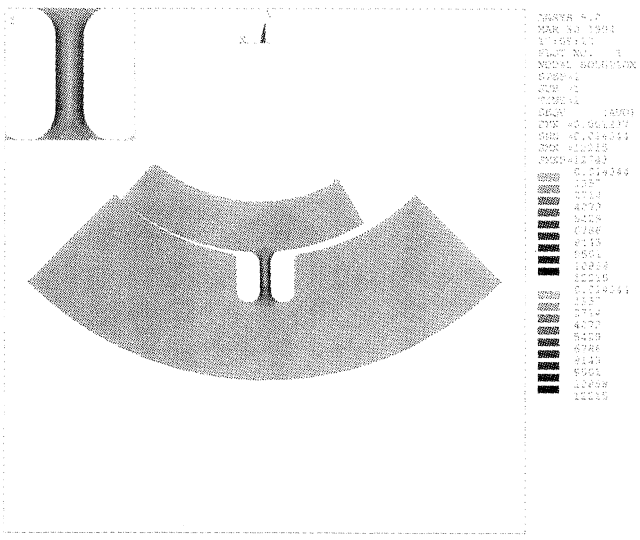

Figure 18. Finite Element Stress Analysis Contours for the Flexure Pivot Bearing.

An obstacle that has played a role in slowing acceptance of the FPB bearing is the relatively thin web feature. This thin structural member often leads to concerns about the stresses and the fatigue life of the web. These fears have prompted the detailed analysis of the stresses and fatigue limit, as shown in Figure 19. The modified Goodman diagram confirms that the bearing has a substantial margin of safety and that the stresses are well below the endurance limit of the structural material. In fact, the stresses are much lower than the contact stresses at the interface between the shell and the rocker back tilt pad in conventional tilt pad

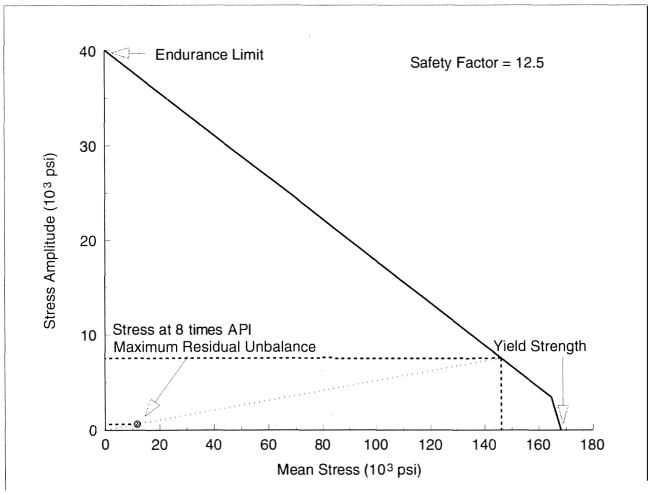

Figure 19. Modified Goodman Diagram for the Flexible Pivot Bearing.

bearings. Furthermore, there is no wear or fretting with the flexible pivot bearings. This ensures that the performance will be maintained regardless of how long the bearings are in service.

There is a striking similarity between the slow acceptance of the flexible pivot bearings and dry flexible element couplings. The analogy centers around concerns raised about the stresses, fatigue life, and endurance limit of the thin web section. However, the amount of pad tilt that actually takes place once the shaft is positioned in the bearing is very small. This is because once the shaft is in place within the bearing clearance, it will limit the maximum amount of pad tilt. As a result of this physical limit, the stresses will be very low. On the other hand, a clear distinction between flexible element couplings and flexible pad bearings lies in the mode of bending that occurs. Unlike the flexible element coupling, the flexible pad bearing does not undergo reverse bending. The pad is tilted in one direction due to the static load, and experiences only small oscillations about the steady state tilt position, due to the dynamic unbalance load.

Another advantage the flexible pivot bearings have is the relatively high radial stiffness. The pivot stiffness of this bearing and conventional style bearings are shown in Figure 20. Note that in the case of the flexible pivot bearing, the stiffness remains constant as the load changes. This is very attractive in the case

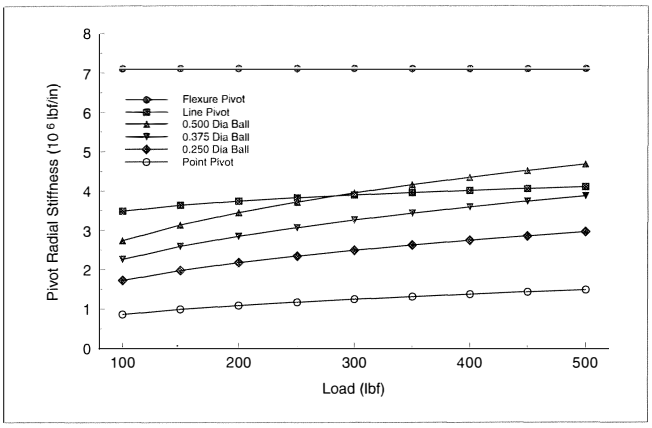

Figure 20. Comparison of Pivot Radial Stiffness for Various Pivot Geometries.

of integrally geared compressors where the bearing gear load changes with compressor load. Finally, bearings used in gear loaded applications represent a class of bearings that are subjected to the most demanding duty. The bearing unit loading typically ranges from 280 to 400 psi compared to 50 to 200 psi for conventional gravity loaded compressor applications. The flexible pivot bearing has proven to be better capable of handling these high loads (stresses) and speeds (30,000 to 80,000 rpm). This bearing design, unlike conventional tilt pad bearings, does not shift the weak link in the bearing from the babbitt to the pivot.

THRUST BEARING ANALYSIS

Fixed Geometry Bearings

The most common type of thrust bearings used in high speed compressors are taper land, Rayleigh step, and pocket bearings. These bearings are simple to manufacture and do not require a wide axial space. The requirement for a narrow axial space is very critical with high speed compressors in order to maintain high shaft rigidity. However, fixed geometry bearings are not capable of handling misalignment conditions. Consequently, this limitation with the fixed geometry bearings demands an over-designed bearing in order to account for the lack of misalignment capability. As a result, the bearing design is far from optimum and a significant frictional power loss takes place.

Variable Geometry Bearings

Self-leveling tilting pad thrust bearings can accommodate misalignment, but this is done at the expense of a relatively large axial space. Therefore, they are not considered as a viable option with high speed integrally geared compressors. Nonequalized tilt pad thrust bearings will require high precision due to the variation in manufacturing tolerance, and at high speeds, the inactive bearing will often experience pad flutter.

Flexible pivot thrust bearings offer a valuable alternative which is very well suited for these types of applications. The tilting motion and convergent wedge is achieved through the flexure of the pad top and of the post. The capability of including the structural finite element model of the pad into the finite element solution of the Reynolds lubrication equation, provides an accurate means of evaluating the performance characteristics of the thrust bearing. Including the crowning of the pad top under load allows optimization of the crown-to-minimum film thickness ratio. This will allow the pad to carry higher loads without sacrificing performance or reliability. The APPENDIX includes a derivation of the analysis routine used to analyze flexible pivot thrust bearings.

FLEXIBLE PIVOT THRUST BEARING DESIGN

The flexible pivot thrust bearings being discussed utilize the elastic deformations of the bearing structure to provide the converging wedge. In most oil lubricated bearings, the minimum film thickness is on the order of one mil. Since the optimum wedge ratio for a tilt pad bearing is around 2.5, this translates to a leading edge tilt or deflection on the order of 2.5 mils. Therefore, the thrust pad does not have to deflect much in order to provide optimum performance. Consequently, the stresses are very low and small compared to the contact stresses in a conventional tilting pad pivot bearing. Adequate safety margins exist in this bearing design to maintain a high degree of reliability.

The bearing performance characteristics are arrived at by solving the Reynolds and energy equations using a finite element formulation [2] that accounts for the structural properties of the pad. The mechanical and thermal deformations of the thrust pads are included in the analytical model [3]. Including

mechanical and thermal deformations is critical to an accurate determination of the film thickness, wedge ratio, and power loss, etc. These effects are often ignored in conventional bearing analysis and, as a result, the information on the pad crown profile is not known. In thin section bearings and in large pads, the ability to model the pad structural and thermal deformations is of paramount importance, since this has a significant influence on the crown profile. An excessive crown profile, as shown to the right of the shaded region in Figure 21, results in lower load carrying capability. The shaded area represents a region of optimum performance where the crown height-to-film thickness ratio can be optimized for higher load carrying capability and lower power loss. The stress and temperature distribution along the surface and throughout the pad are also provided by the analysis and allow an accurate determination of the stress levels and safety factors.

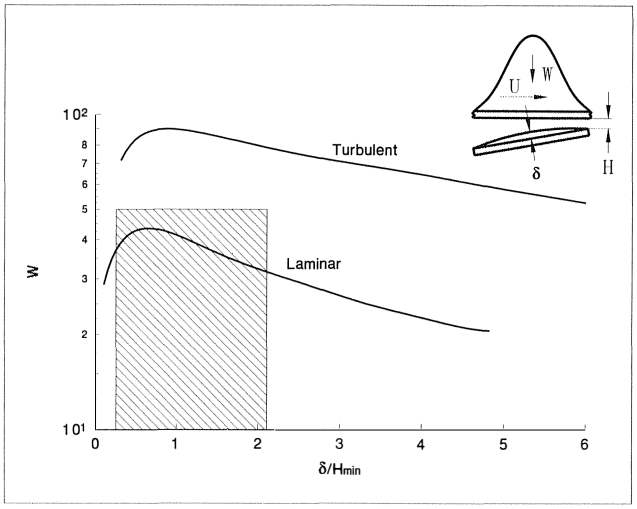

Figure 21. Effect of Film Thickness to Crown Ratio on the Load Carrying Capacity.

The thrust bearing in this configuration is designed to carry a load of 200 lb at 76,500 rpm when only one impeller stage is used. When two impellers or two stages are utilized, the maximum thrust load is around 100 lb. As mentioned earlier, the desired maximum speed in the future will be increased by 20 to 30 percent over the current speed. The thrust pads are made of a bearing grade copper alloy that has excellent thermal conductivity. This will aid in carrying the heat away from the oil film.

A finite element model of the thrust pad is shown in Figure 22. The pad has an offset pivot to provide lower power loss and higher load carrying capability. The circular pad geometry is selected for ease of manufacturing (turning), and because the surface area did not have to be maximized. The power loss and minimum film thickness as a function of load at 76,500 rpm are shown in Figure 23. The stress contours in the pad under load are shown in Figure 24. The maximum stress is 17,800 psi which results in a safety factor of 7.9.

A six pad thrust bearing was optimized to meet the design requirement of 200 lb thrust load at 76,500 rpm. The pads are assembled in the carrier with an additional height stock allowance. The pads are then ground and lapped as an assembly, thus eliminating the stackup of manufacturing tolerances associated with individual components. The carrier was designed to reduce the parasitic losses which are difficult to calculate but can be deduced from the test measurements.

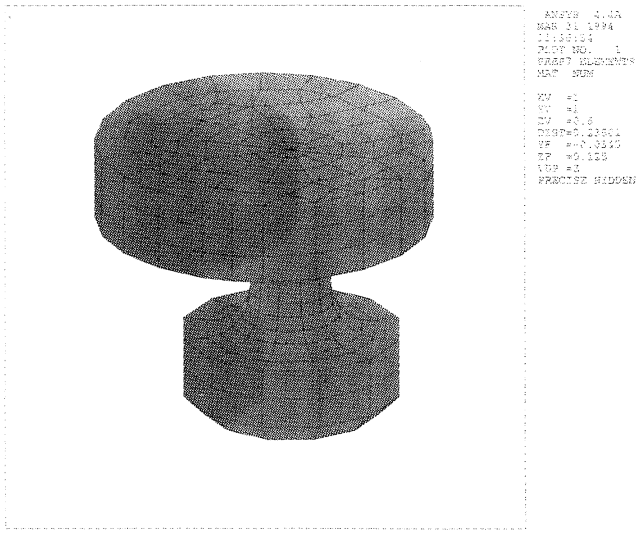

Figure 22. Finite Element Model of the Thrust Pad.

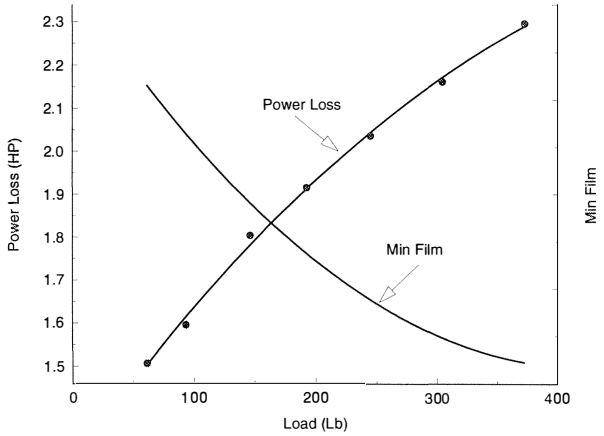

Figure 23. Flexible Pivot Thrust Bearing Power Loss and Film Thickness as a Function of the Load.

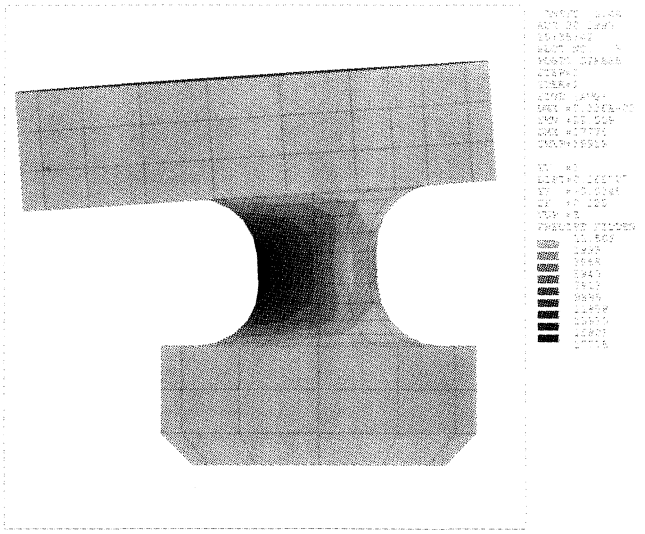

Figure 24. Finite Element Stress Contour Plot of the Thrust Pad.

Table 3. Comparison of Thrust Bearing Predicted Power Loss at Test Conditions. Speed = 76000 rpm; load = 100 lb; oil inlet temp = 160°F; and flowrate = 2 gpm.

Bearing Type			*Power Loss (HP)*
TPB (Baseline)	Active	Pocket	1.72[1]
	Inactive	Taper/Land	2.86
	Total		4.58
FPB	Active	Flex Pivot	1.67
	Inactive	Flex Pivot	1.05
	Total		2.72
Difference			1.86

A predicted power loss comparison of the TPB (baseline) thrust bearing to the FPB thrust bearing under the test conditions is presented in Table 3. The power loss of a FPB bearing is 40 percent lower than the power loss expected of the existing TPB (active-pocket and inactive-taper/land) thrust bearing. Since there is no improvement in the power loss due to the FPB radial bearing, and the power loss in the gear system is expected to be the same for the TPB and FPB system, any power loss saving can be attributed to the FPB thrust bearings. The experimental observations, which are discussed in the next section, show that the average power loss saving of the FPB compared to the TPB is 2 to 2.5 HP. This correlates well with the analytical predictions.

BEARING TESTING AND EVALUATION

Test Procedure and Layout

The testing of the bearing was performed at the OEM's test facility using a production compressor. A schematic layout of the instrumentation plan is shown in Figure 25. Eddy current proximity probes were used to measure shaft vibrations. Temperature sensors and flow meters were used to measure the lubricant temperature to and out of each bearing and the corresponding oil flow. The temperature rise and the oil flow rate were used to calculate the power loss in the journal and thrust bearings. The compressor uses MIL-7808, a synthetic oil for lubricating the gears and bearings. For the purpose of this investigation, the oil piping and controls have been slightly modified. The temperature regulating valve located upstream of the oil pump was disabled, and a control valve was installed in the hot oil line parallel to the oil cooler line. This allowed the oil inlet temperature to be varied. The oil pressure relief valve was completely closed to maintain the same oil flow to the compressor as indicated by the dotted line in Figure 25. A constant oil flow of 8 GPM was maintained throughout the test. The auxiliary driven prelube pump was on only during startup, shutdown, and idle time after a shutdown for cooling purposes. When the compressor reached operating speed, the main oil pump driven by the bull gear supplied oil to the bearings. Two separate flow meters were located at the feed to each bearing. Numerous thermocouples were installed at various locations for temperature measurements. This arrangement allowed determination of the power losses in each combination radial/thrust bearing, and across the entire compressor train. The oil inlet temperature to the compressor was varied by adjusting the hot oil flow control valve parallel to the cold oil through the oil cooler. The total power loss (frictional plus parasitic) was calculated using Equation (1).

$$hp = 0.1967 \cdot gpm \cdot density \cdot C_p \cdot \Delta T \qquad (1)$$

where,

hp	power loss (hp)
0.1967	a units conversion constant
gpm	flowrate (gpm)
density	fluid density (g/cc)
C_p	fluid specific heat (BTU/lb/°F)
ΔT	average temperature rise (°F)

The configurations of the three bearings tested are listed in Table 4. The third configuration is the same as the second with some minor changes to the thrust bearing carrier in order to reduce the parasitic losses.

Table 4. Bearing Configurations Tested.

Design Cases	Stage 1		Stage 2	
	Radial	Thrust	Radial	Thrust
Design 1 - TPB	Tilt Pad	Taper Land	Tilt Pad	Pressure Pocket
Design 2 - FPB	Flex Pad	Flex Pad	Flex Pad	Flex Pad
Design 3 - FPB	Flex Pad	Flex Pad	Flex Pad	Flex Pad

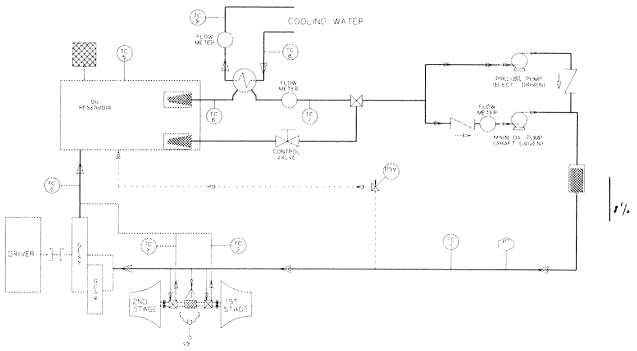

Figure 25. Schematic Layout of the Test Instrumentation.

Vibration Measurements

The vibrations were measured using an eddy current proximity probe system. The data was then processed through a frequency spectrum analyzer. The steady state vibration frequency spectra for the tilt pad and flexible pivot bearings, superimposed on the same plot, are shown in Figure 26. As predicted in the unbalance response analysis shown in Figure 17, the response with the flexible pivot bearing is about 50 percent lower than with the conventional tilt pad bearing. Furthermore, the tilt pad bearing had lower damping as evidenced by the subsynchronous components present in the frequency spectra.

Vibration data were also recorded during a surge cycle of the compressor. The subsequent vibrations spectra for both bearing types, superimposed on the same plot, are shown in Figure 27. Note that in this case too, the vibrations with the conventional style tilt pad bearing were higher and increased much more than the vibrations with the flexible pivot bearings. These bearings did not show any change or increase in subsynchronous vibrations, whereas there was a significant increase with the tilt pad bearings.

Measurements of Bearing Power Loss

The temperature rise was measured for the bearings corresponding to each of the two compressor stages. These measure-

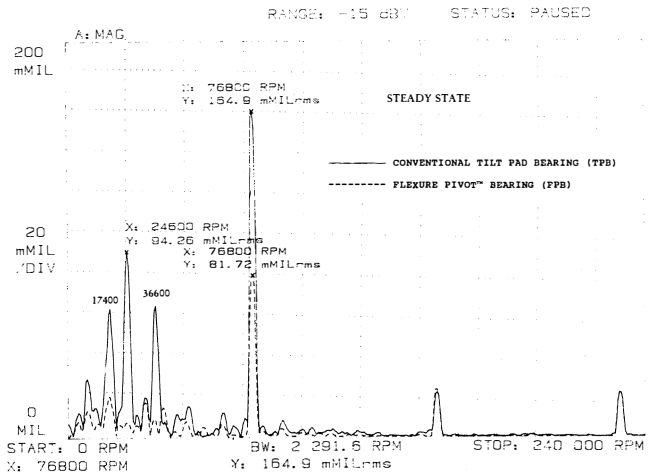

Figure 26. Steady State Vibrations for the Tilt Pad and Flexible Pivot Bearings.

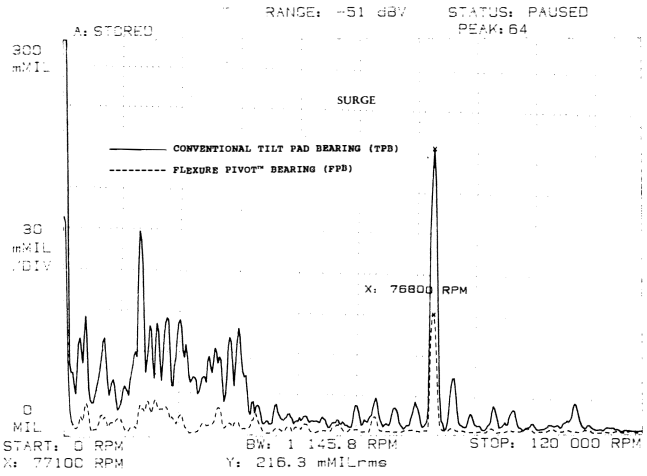

Figure 27. Vibrations Measured Under Surge Conditions for the Tilt Pad and Flexible Pivot Bearings.

ments were made while the oil inlet temperature was varied. Each data point was obtained after allowing all the measurement variables to reach steady state conditions. The results with both bearings are shown in Figure 28. The first stage bearing was subjected to the higher thrust load and, therefore, had the higher temperature rise. In both stages, the flexible pivot bearings experience lower temperature rise in comparison to the pocket and taper land thrust bearings. The oil outlet temperature as a function of the oil inlet temperature is shown in Figure 29. This confirms that the oil inlet temperature can still be increased to induce a further reduction in the power loss without reaching the maximum outlet temperature limit. The total power loss which includes the first and second stage journal and thrust bearings is shown in Figure 30. There is about a 2.5 HP savings with the FPB bearings in comparison to the conventional tilt pad bearings.

The first flexible pad thrust bearing carrier, shown in Figure 7, had sharp edges between pads. This configuration did not lend itself to reducing the parasitic losses. Parasitic losses, as reported by Booser and Missana [4], can account for 25 to 50 percent of the total bearing fluid power losses. The second flexible pivot thrust bearing eliminated some of the sharp edges and provided a more directed lubrication configuration. The results for all three bearing configurations can be seen in Figure 31. Since the

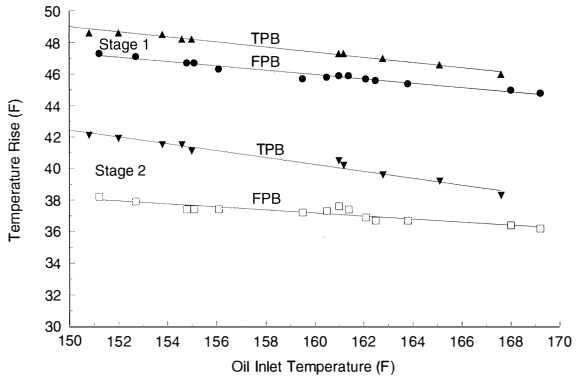

Figure 28. Measured Oil Temperature Rise as a Function of Oil Inlet Temperature.

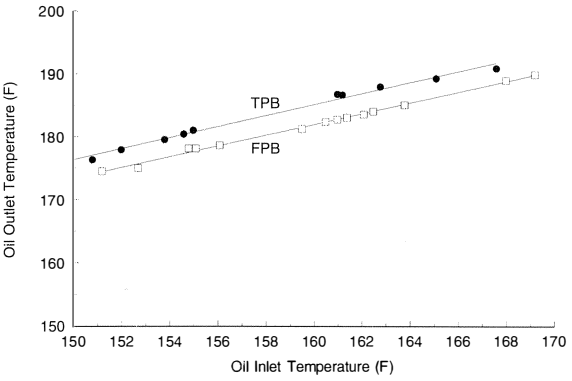

Figure 29. Oil Outlet Temperature as a Function of Oil Inlet Temperature.

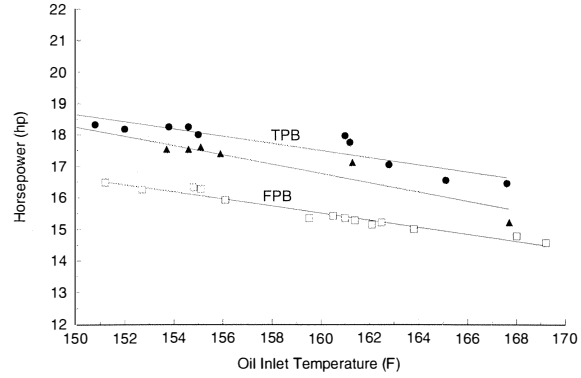

Figure 30. Power Loss as a Function of Oil Inlet Temperature.

flexible pivot thrust and journal pads were identical to those in the first configuration, the reduction in the power loss noted between the two flexible pivot bearings can be totally attributed to the effect of the parasitic losses.

CONCLUSIONS

The vibration characteristics with the flexible pivot bearings showed improvements over the conventional style tilt pad bearings during normal steady state operation and under surge conditions. The precision with which the flexible pivot bearing is manufactured, gives it a distinct advantage over conventional style tilt pad bearings. This is because the stackup in tolerances

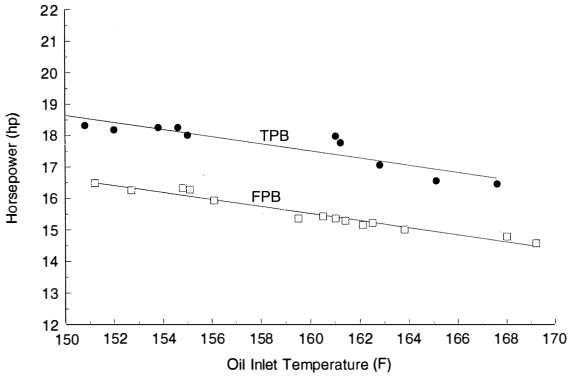

Figure 31. Power Loss as a Function of Oil Inlet Temperature for All Three Tested Bearings.

with conventional style tilt pad bearings results in a very wide range for the clearances and preload.

The use of an offset pivot in this application showed that the journal bearing can run 20 to 30°F cooler. The offset pivot design also showed advantages that were not clearly identified in the literature. The bearing sensitivity to clearance variations with an offset pivot was demonstrated to have a limited influence on the stability. The cross coupled stiffness for the 0.5 and 0.6 offset bearing as a function of the flexure pivot rotational stiffness is shown in Figure 32. The difference in the cross coupled stiffness between the 0.5 and 0.6 offset is negligible. The distinct difference, however, can be seen when the principle stiffness is plotted for both offset positions as a function of rotational stiffness, as shown in Figure 33. As the rotational stiffness in the pads approach the variable geometry (tilting) region, there is a dramatic increase in the direct stiffness with the 0.6 offset pad configuration. What is of even more significance is the increase in damping for the 0.6 offset pads, as shown in Figure 34. The increase in stiffness and damping is responsible for the reduction in sensitivity with variation in bearing clearance and for the higher logarithmic decrement predicted with the offset pivots.

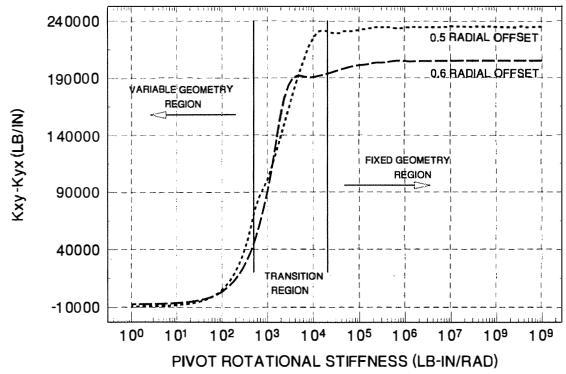

Figure 32. CrossCoupled Stiffness (Kxy - Kyx) as a Function of FPB Rotational Stiffness.

This investigation also confirmed that parasitic losses form a substantial part of the overall power losses in a bearing. The FPB bearing design reduced the frictional and parasitic losses by 2.0 to 2.5 hp. More importantly, the design of the flexible pivot bearing enables incorporating features in the thrust bearing, which can reduce the parasitic losses. Subsequently, the parasitic losses were reduced by an additional 1.0 to 1.5 hp.

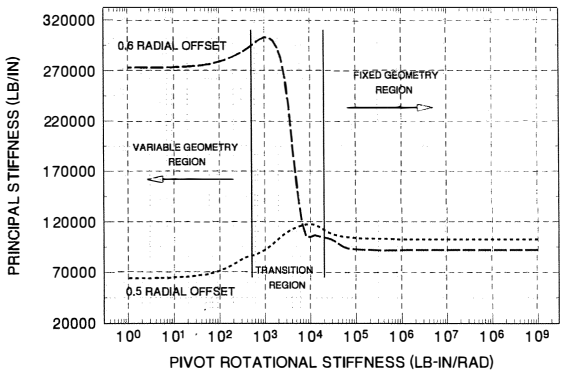

Figure 33. Principal Stiffness (Kxx, Kyy) as a Function of FPB Rotational Stiffness.

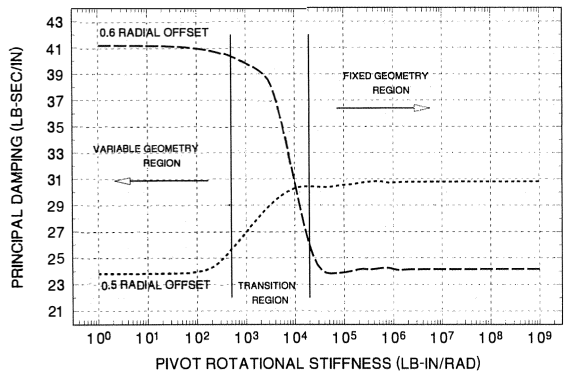

Figure 34. Principal Damping (Cxx, Cyy) as a Function of FPB Rotational Stiffness.

APPENDIX—DESIGN AND ANALYSIS OF FPB THRUST BEARINGS

In a conventional fixed geometry fluid film bearing design, such as a taper land or a Rayleigh step bearing, the converging geometry is generated by machining the bearing surface to provide a converging wedge. A tilting pad bearing on the other hand, through its ability to tilt and form a convergent wedge geometry is classified as a variable geometry bearing. The flexible pivot bearing falls in the same category as the tilting pad bearing due to its ability to flex and tilt, thus forming a variable geometry wedge. In the flexible pivot bearing, the hydrodynamic pressure developed in the fluid induces the pad top and the flexible pivot to elastically deform. This deformation forms the converging wedge-shaped gap between the bearing surfaces.

The primary objective in the design of a flexible pivot bearing is to optimize the deformation of the bearing components, within the structural limits of the material. The differential equation governing the pressure in the fluid film is the Reynolds lubrication equation. Solving the Reynolds equation and accounting for all the factors which influence the performance characteristics is a very involved procedure. In many of the conventional bearing designs, factors such as the changes in the fluid temperature and viscosity, pad mechanical and thermal deformations, etc., are neglected. Flexible pivot bearings, on the other hand, address these effects and use them to advantage in order to generate an optimum pad profile and develop a higher load carrying capability. In a flexible pivot bearing design, a numerical solution to the Reynolds equation is obtained, followed by an energy balance calculation, and a structural elastic deformation analysis. These

analysis steps are coupled and solved in an iterative manner. The following outlines how the design process is executed:

- Estimate the initial fluid film thickness between the bearing surfaces based upon the geometry and the operating conditions.
- Solve the Reynolds equation and calculate the pressure distribution on the pad, the power loss, the temperature rise, and the variations in the fluid properties along the pad.
- Calculate the pad structural deformations due to the fluid pressure and temperature.
- Update the fluid film thickness as a result of the structural deformation.
- Repeat steps two through four until an equilibrium is reached.
- Calculate the stresses in the bearing under the equilibrium pressure.

A structural analysis to determine the pad deformation is required during every iteration, because the pressure distribution changes in every iterative step. The ANSYS® finite element analysis program is used to perform the structural analysis. KMC® proprietary programs are used to perform the fluid dynamic analysis of the thrust and the radial bearings. The fluid dynamic and the structural analyses are coupled by the use of a structural compliant matrix.

Each element a_{ij} in the square, symmetric structural compliant matrix represents the displacement of nodei due to a unit load applied at nodej. Only the nodes on the pad top constitute the domain of the compliant matrix which helps considerably in reducing the problem size. The displacement analysis used to generate the compliant matrix consists of creating the finite element model of the entire pad structure. This is followed by applying a unit load to a node on the pad top, performing an ANSYS® displacement analysis, and extracting the resultant displacements of all the nodes on the pad top surface. The analysis is repeated for all the nodes on the pad top surface.

The fluid dynamic analysis program uses a finite element algorithm to solve the Reynolds lubrication equation. The location of the nodes in the finite element lubrication program matches the location of the nodes generated in the structural program. The program follows the steps outlined above and uses the compliant matrix to calculate the pad deformations. Finally, the calculated equilibrium pressure is applied to the finite element structure of the entire pad to obtain the resulting stresses throughout the pad.

REFERENCES

1. Japikse, D. and Olsofka, F. A., "Agile Engineering: A Look at Tomorrow," Proceedings of ROCON-93 Rotating Machinery Conference and Exposition, *1*, Somerset, New Jersey (1993).
2. Reddi, M. M., "Finite-Element Solution of the Incompressible Lubrication Problem," Trans. ASME, Journal of Lubrication Technology, *91*, Series F, (3), pp. 524-533 (July 1969).
3. Jain, D., "Parametric Design of Deflection Pad Bearings," ANSYS 1992 Conference Proceedings, *I*, pp 1.31-1.39 (1992).
4. Booser, E. R. and Missana, A., "Parasitic Losses in Turbine Bearings," Tribology Transactions, *33* (2), pp 157-162 (1990).

ACKNOWLEDGEMENTS

The authors wish to thank Patrick Powers, Russ Houston, and Frank Olsofka of Ingersoll-Rand for their support and help. Thanks are also due to Christian Paraskevakos and Robert Ramsay of KMC for producing some of the figures and reviewing the paper. The authors would also like to thank their respective companies for permission to publish this paper.